Responses to the Reviewer 1

The authors of the submitted research analyse with mathematical/statistical tools published seismic event catalogues from areas of high seismicity (Taiwan and Japan) in an attempt to identify patterns in the distribution on time and space of foreshocks of larger events. The presented results point to a distribution much wider of the foreshocks in time (up to 60 days) and space (up to 400 km of the main shock epicentre) of those currently accepted, even for main shocks of moderate magnitude. Such kind of analysis is promising; but I think as performed and presented in the submitted research is not yet ready for publication.
To me, it looks like the pieces of the submitted paper have been assembled in a hurry. The used methodologies need more explanation (why and how they are applied). Even more comments on the choice of the data are also needed. Moreover, a revision of the English syntax is needed. The sense of phrases is difficult to follow in many cases.

For these reasons I think the submitted research needs a deep and throughout revision before it can be accepted for publication.
In the following paragraphs I point some specific questions to be addressed on the submitted text.

-Methodology- Line 85. Citation Chen (2014) is not in the reference list.
Reply:
The correct reference is Chang (2014) and has been cited in the manuscript. (Line 96)

Lines 87-89. It is necessary to introduce a minimum description on how ZMAP software removes aftershocks.
Reply:” The ZMAP software package for MATLAB (Weimer, 2001) was utilized to remove and/or omit influence from duplicate events, such as aftershocks.” has been rewriten as “To distinguish dependencies from independent seismicity, the earthquake catalogs are declustered. Therefore, the ZMAP software package for MATLAB (Weimer, 2001) was utilized to remove and/or omit influence from duplicate events, such as aftershocks. The declustering algorithm used in ZMAP is based on the algorithm developed by Reasenberg (Reasenberg, 1985).” (Lines 98-102)

Lines 89-95. Idem: a minimum description on how clusters are classified and the meaning of the input parameters is necessary.
Reply:” We classify clusters by using the standard input parameters (proposed in Reasenberg, 1985 and Uhrhammer, 1986) for declustering algorithm. The minimum and maximum values of the look-ahead time for building clusters are 1 and 10, respectively. The probability of detecting the next clustered event used to compute the look-ahead time is 0.95. The effective minimum magnitude cut-off for catalog is given by 1.5 and the xk factor for the increase of the minimum cut-off magnitude during clusters is given by 0.5.” has been rewriten as “We classify clusters by using the standard input parameters (proposed in

Reasenberg, 1985 and Uhrhammer, 1986) for the declustering algorithm. Because the aftershock clusters in a small area and in a short period of time do not conform to the Poisson distribution, which requires removing the aftershocks from the earthquake sequence. Therefore, some parameters can be set as follow: The look-ahead time for un-clustered events is in one day, and the maximum look-ahead time for clustered events is in 10 days. The measure of probability to detect the next event in the earthquake sequence is 0.95. The effective minimum magnitude cut-off for the catalog is given by 1.5, and the interaction radius of dependent events is given by 10 km (van Stiphout et al., 2012)." (Lines 103-111)

Line 95. "The 10 of crack radii: : :" Do you mean 10 times the crack radii? Please, make clear this phrase.

Reply:

Sorry for the ambiguous statement, the sentence is indicated as the interaction radius of dependent events is given by 10 km. The modified description is listed at lines 110-111.

Line 96. Cite Stiphout (2012) is missing in the reference list.

Reply:

The reference has been added in the list.

van Stiphout, T., J. Zhuang, and D. Marsan (2012), Seismicity declustering, Community Online Resource for Statistical Seismicity Analysis, doi:10.5078/corssa52382934. Available at http://www.corssa.org.

Lines 99-102. If I understand properly "crack" and "break" events are definitions you introduced in your analysis, being "crack events" quite equivalent to foreshocks and aftershocks. Please, make clear all these terms.

Reply:

Sorry for the confusion. The "crack" and "break" events have been defined in the manuscript in lines 114-125. Note that we assumed the break event is an earthquake. The crack events can be foreshocks and aftershocks. We stack the crack events to the break events by the time and spatial distance to examine their relationship.

Lines 102-104. There is some problem with the minimum completeness magnitude of the catalogues. Looking at figures S1-S4 it looks like the events in the Taiwan catalogue are included in the Japanese catalogue. Something should be said about this fact. Moreover, the Japanese catalogue comprises many events far away from the main islands (23-34N, 138-147E). I think this whole region does not have the dense seismometer network claimed in lines 83-85. All these points should be clarified in the text.

Reply:

Thank you for your comments. We have modified the results of the Japan catalogs by using the earthquakes that occurred in the northern side of the latitude of 32°N to mainly concentrate in areas with the dense seismometer network and to avoid the double counts of earthquakes in the Taiwan catalogs (lines 187-191). This result is consistent with the previous results, but in order to avoid the problems raised by the reviewer, the revised version will be based on this result. (also see Figs. 1 and 2 in the revision)

Lines 109-110. I assume the spatial and temporal resolutions of the grid are a choice of the authors. If so you may comment if you try other resolutions and/or the reasons for your choice.

Reply:

Sorry for the confusion. The statements have been revised as "Note that the spatial and temporal resolutions of the grids of the spatiotemporal distribution are 10 km and 1 day, respectively, based on the declustering parameters in the ZMAP software." (lines 130-132). Note that the statements associated with the declustering parameters also used in the ZMAP software and the declustering process in ven Stiphout et al., (2012) and Zare et al., (2014). (Lines 107-111)

Reference

Zare, M., Amini, H. and Yazdi, P.; Recent developments of the Middle East catalog, J. Seismol., 18, 749–772, 2014. https://doi.org/10.1007/s10950-014-9444-1.

Lines 113-116. The superimposition process statistical tool should be described. It is not a common tool in seismicity studies.

Reply:

The associated statements have been revised and added for clarification.

In practice, the superimposition is a process to stack numerous datasets that can migrate unique features for a few datasets and enhance common characteristics for the most datasets. The count in each grid of the spatiotemporal distributions for all the break quakes are superimposed as a total one based on the occurrence time and epicentral distance of the break quakes. (Lines 138-143)

Lines 118-121. It is not clear to me what "migrate rare characteristics" means. Please clarify this phrase.

Reply：

The associated statements have been revised as "In practice, the superimposition is a process to stack numerous datasets that can migrate unique features for a few datasets and enhance common characteristics for the most datasets.". (Lines 138-140)

-Analytical Results-

Lines 130-132. All M2 events are foreshocks or aftershock of M3 events? Cannot they be independent events?

Reply:

This is a very interesting comment. Initially, the opinion from the authors are the same with the reviewer. M2 events can be foreshocks or aftershock of M3 events. Meanwhile, the authors understood that the ZMAP may not fully remove the influence from M2 aftershocks. In fact, we analyze the data without any assumption except for taking the break event as an earthquake.

Here, we made the artificial events as the break events for the tests based on that the relationships between the artificial and break events are (1) independent in the time and spatial domain; (2) time dependent (i.e., the same occurrence time but distinct location); (3) location dependent (i.e., the same occurrence location but distinct time). These results are processed by using the same method to construct the spatiotemporal seismic density distributions and the spatiotemporal normalized variations in Figs. A and B (in below) for comparison. No significant increase of the seismic activity can be observed in Figs. 1b-d and 2b-d for the artificial events. In contrast, we can find increase of the seismic activity in Figs. 1a and 2a. This suggests that M2 events could related to the M3 events with a variable distance along the time. (Lines 161-175).

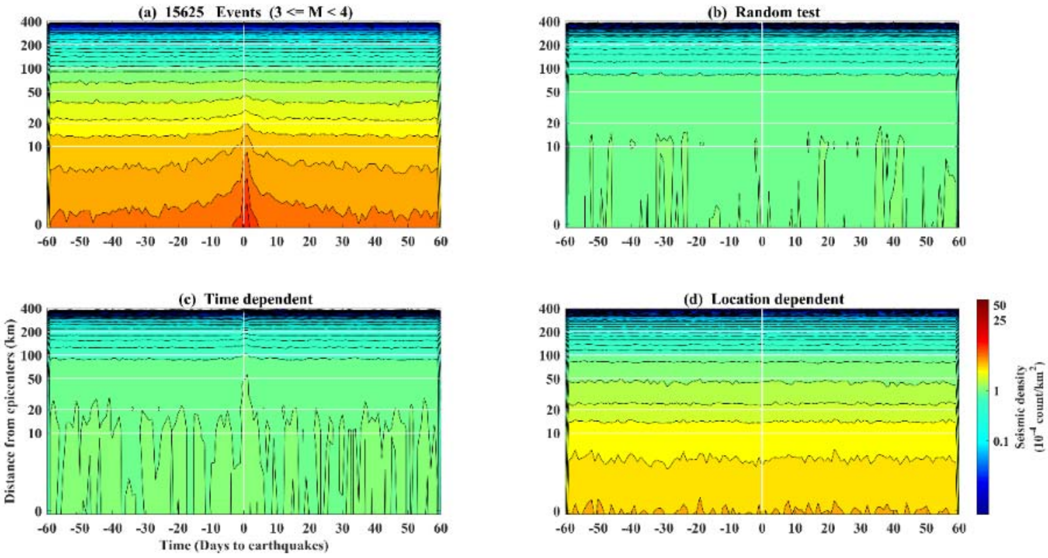

Fig. A. Spatiotemporal seismic density distributions in Taiwan. (a) is computed by the M2 events relate to the real M3-4 events. (b) is computed by the M2 events related to the random M3-4 events in the time and frequency domain. (c) is computed by the M2 events related to time dependent M3-4 events. (d) is computed by the M2 events related to location dependent M3-4 events.

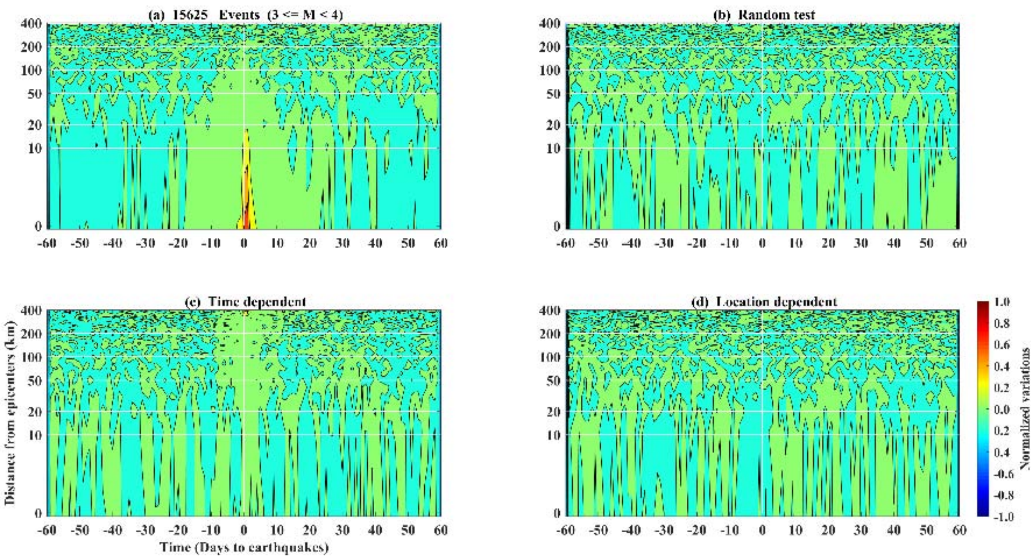

Fig. B. Changes of spatiotemporal normalized variations in Taiwan. (a) is computed by the M2 events relate to the real M3-4 events. (b) is computed by the M2 events related to the random M3-4 events in the time and frequency domain. (c) is computed by the M2 events related to time dependent M3-4 events. (d) is computed by the M2 events related to location dependent M3-4 events.

Lines 132-134. What does it means that S/N ratio increases 135 times? Please clarify.

Reply:

The associated statement has been removed.

Another issue: 17993 M3 events in the period 1991-2017/6 mean 2 events per day roughly. As Taiwan is 400 km long approx., it means that in a period of 60 days and 400 km as you are using in your analysis. there are many M3 earthquakes (100 approx.). It is not clear to me how the M2 events are associated with the M3 events. Maybe a good description of the superimposition process as applied in this case clarifies this issue.

Reply:

Thank you for your comments. Those M3 events do not occur in the same region. Instead, the M3 events widely distributed in Taiwan and Japan areas. The distances between the M2 and M3 events are utilized as an important parameter in this study. The distances from the M2 to the distinct M3 events are different. This suggests if the relationship does not exist that can be mitigated through the stacking processes due to the distinct spatial distribution dominated by the diffident distances (also see Figs. A and B). In contrast, if the relationship dose exist, it can become obvious after the stacking of more than 10 thousand of the M3-4 events. The authors have rewritten the statements associated with the superimposition process in lines 138-143.

Lines 145-164. The previous pointed issues make difficult to follow the discussion on the results.

Reply:

Sorry for the confusion. In this paragraph, the authors focus on the areas with the increase of seismicity density before earthquakes that extends from the fault rupture zone to an external place. The associated statements have been written in the manuscript (Lines 175-212).

-Discussion- In fact this section presents a different analysis, using seismograms and the PCA method. Certainly, the presented analysis has been inspired by the results obtained in the previous section; but it can be performed and presented in a totally independent form. Thus, it should be better presented as another section of analysis results. It is not clear how you are using the PCA analysis in this case. Some figure showing an example of the procedure described on lines 217-222 can help.

Reply:

The statements associated with the descriptions and results associated with the PCA have been move to the new section of the principal component analysis (PCA) on the continuous seismic waveform in lines 234-248. Figure 3 has been added to reveal the energy of the principal components and the first principal component retrieved from continuous seismic waveforms at 31 stations. Figure S5 have been moved to the main text as Figure 4. Note that Figure 4a shows that the amplitude ratio associated with the Meinong earthquake without the superimposition or the stacking process. For the superimposition or the stacking results associated with the M4-5 and M3-4 earthquakes are shown in Figs. 4b and 4c.

Lines 237-246. There are a lot of suppositions on the used dimensions. If horizontal dimensions (100 x 100 km2) can be roughly deduced/assumed from the previous results (obtained in this section and the previous one), the thickness between 500-1000 m needs a good explanation.

Reply:

The authors appreciate that the reviewer can accept the area in the horizontal dimensions. If the resonance model in the manuscript is true, the unknown parameter of the stress plate is the thickness. The area in the horizontal dimensions is given by the observation in this study. The resonance frequency is obtained by the results of continuous seismic waveforms. The thickness between 500-1000 m is obtained based on the resonance model. The authors just propose a potential model to connect the wide area of increase of seismic activity and the frequency characteristics of crustal vibrations. The authors do not have any evidence to support the thickness between 500-1000 m. In fact, the thickness of the seismogenic areas is smaller than it of the crust that can be one of the candidates of potential causal mechanism. The authors understood that the debate of the resonance model cannot be solved immediately. We have shortened the statements associated with the resonance model. The original Fig. 4 has been moved to the supplementary for references.

Lines 275-276. I cannot see the need for this citation here. Even more, I has been unable to find the value 2700 km/m^3 in the cited paper or on the additional information.

Reply:

The reference has been removed from the manuscript.

Responses to the Reviewer 2

The manuscript presents results which, in my opinion, can be very relevant for the forecasting challange. However I find that they are not well presented and the discussion appears quite confusing for the following reasons:

The first part of the manuscript is devoted to study spatio-temporal patterns of seismic activity before and after events in a given magnitude range, for Taiwan and Japan. There are many papers which report a similar increase of seismic activity before large earthquakes. The key point is if the observed increase can have a prognostic value or it can be explained within normal aftershock triggering.

Reply:

The authors fully agree with the comment. The results for the increase of seismic activity close to the epicenter observed in Figs. 1 and 2 are consistent with the observation in the previous studies (Lippiello et al., 2012, 2017, 2019; de Arcangelis et al., 2016). The associated statements have been added in the manuscript (lines 171-174). The agreement suggests that the increase of seismic activity in Figs. 1 and 2 is not contributed by aftershocks but a prognostic value.

I just suggest some papers where this point is detailed discussed, other references can be find therein (Lippiello et al., Scientific Reports 2012, de Arcangelis et al. Physics Reports 2016, Lippiello et al., Pure and Applied Geophys. 2017, Lippiello et al., Entropy 2019).

Reply:

Thank you for the suggestions. The authors have added those references in the manuscript for intensely supporting our results (lines 171-174). Meanwhile, we are glad to find that the similar pattern (i.e., sudden increase and gradual decrease of the seismic density before and after the earthquakes) can be confirmed by using the different method.

In my opinion many of the results of sec.3 are not really interesting since they are probably artifact of the adopted stacking procedure. Furthermore they are not strictly related to what for me are the main findings (see my point 2). Therefore, I believe that this section can be moved to the supplementary materials whereas in the main-text the authors can just summarize some results and discussing recent literature on this specific point.

Reply:

Thank you for the comments. The authors have shortened the statements, which is similar with the observation in the previous study (lines 153-174). In fact, the manuscript focuses on the increase of seismicity density before earthquakes that extends from the fault rupture zone to an external place. The associated statements have been extended and added in the manuscript (lines 175-212).

2) Conversely, I strongly encourage the authors to move fig.S5 from the supplementary to the main-text. I am really impressed by this figure. In particular I find striking the result of

the left panel which, if i correctly understand, is for a single M6.6 mainshock and therefore is not contamined by spurious effects caused by the stacking procedure. This figure shows a change in the dominant frequency from roughly 10ˆ{-4}Hz up to 30 days before, to a much larger value before the mainshock.

Reply:

Thank you very much. Fig. S5 has been moved from the supplementary to Fig. 4 in the main text.

What I find really interesting is the analysis at a fixed frequency (around 10ˆ{-4}Hz) as function of the time from the mainshock. In this case you find that the mainshock occurrence time is a minimum" point in the sense that the amplitude ratio at the given frequency decreases before the mainshock and increases after, in a quite symmetric fashion. Comparing with the central panel, which is substantially the same of Fig.3, the authors find a similar pattern at a similar frequency for $4<M<5$ mainshocks. In this case however the decrease of the amplitude ratio before the mainshock and the subsequent increase after is less pronunced. The same holds for $3<M<4$ where the changes of the amplitude ratio are even less pronunced. This is really interesting since it suggests that you can correlate the slope of the amplitude ratio (at a specific frequency) with the magnitude of the incoming mainshock. I invite the authors to focus on this very important result and I suggest some checks to support the scenario.

Reply:

Thank you very much.

i) I don’t fully understand the smoothing procedure: "The common-mode vibration is sliced ....". The really important point is that the amplitude ratio plotted at time t only contains waveforms recorded up to time t. In other words, it is fundamental that quantities evaluated before the mainshock are not contamined by the mainshock signal.

Reply:

Based on the window of 5 days for the slice, the amplitude ratios 5 days before and after earthquakes can be influenced by the mainshock signals. In fact, the enhancements of the amplitude ratios with variable frequency appear more than 20 days earlier than the mainshocks. This suggests that the observed enhancements of the amplitude ratios are not contributed by the mainshock signals.

ii) The authors use the signal from 33 seismometers. What happens if I consider a smaller number? In particular how much results depend on the distance between the seismometer and the mainshock?

Reply

Based on the pre-earthquake crustal deformation and the numerical model in the previous studies, the seismogeneric areas are considered to be larger than the rupture of the fault zone. In addition, Figs. 1 and 2 also show that the increase of seismicity density before earthquakes that extends from the fault rupture zone to an external place. The radius of the areas with the increase of seismicity density is about 50 km for the M3-4 event and is about 150 km for the M5-6 events. The areas of Taiwan Island are very small. This suggests the signals observed in this study can be recorded in the whole Taiwan island.

On the other hand, the upper panel of the Fig. A shows the spatial distribution of amplification ratios in a frequency band between 8 x 10^{-5} to 2 x 10^{-4} Hz for an interval of 0–25 days before the Meinong earthquake. The enhancements roughly cover the whole Taiwan Island. Therefore, the signals can be retrieved from most continuous waveforms from most seismic station. Note that we also take the vertical component of curst displacements from the GNSS data into consideration (the lower panel in Fig. A). An agreement in variations of the spatial distribution of amplification ratios can also be obtained. This suggests that the amplification ratios distribute in areas with epicentral distance > 250 km. Fig. A has been utilized in the paper that is considered for publication in the other journal.

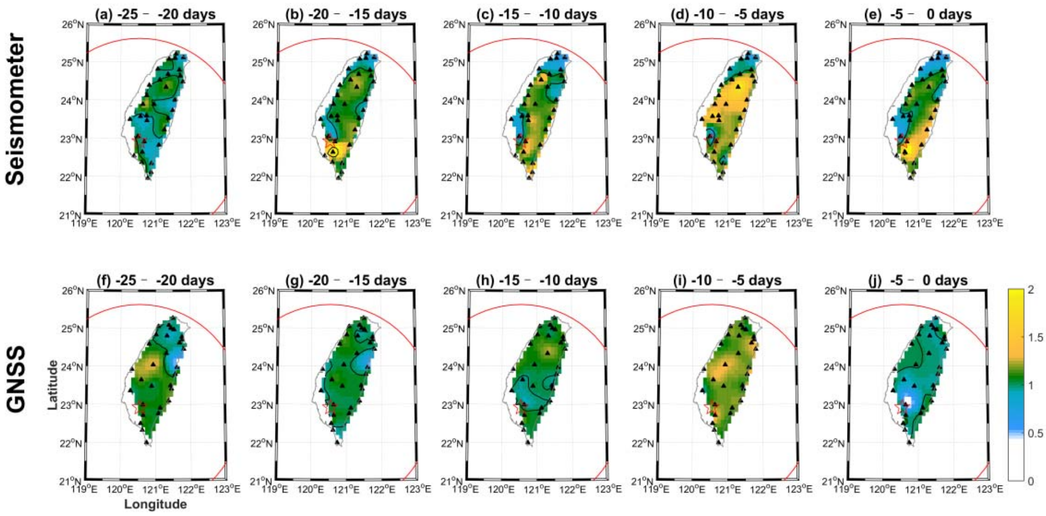

Fig. A. Spatial distribution of amplification ratios computed from seismic and GNSS data for an interval of 0–25 days before the Meinong earthquake. The upper (a)–(e) and lower (f)–(j) panels denote amplification ratios obtained from seismic and GNSS data. The amplification ratio of > 1 (or < 1) suggests enhancement (or attenuation) of ground vibrations in the particular time period. Time intervals for (a)–(j) indicate distinct time spans until the occurrence of the earthquake during which the data were used for the analysis process. The red star denotes the epicenter. The red lines indicate portions of circles with a radius of 300 km from the epicenter of the earthquake.

iii) There is some reason to take the first 20 principal components. What happens if one changes this number?

Reply:

This is a very good question. In the original version, we take the first 20 principal components due to that the threshold of 75% energy is required by other studies. In fact, we can have similar results while the first principal component (12% for energy) is utilized. Note that we have replaced the results in Fig. 4 by using the first principal component in the revision.

iiii) Is there any pattern observed for a single M4+ earthquake, without stacking their signals?

Reply:

Fig. B in below shows the results for a single M4+ earthquake, occurred in the central Taiwan. The enhancements in the frequency between 5x10^{-4} Hz and 10^{-3} Hz can be found that is in agreement with the observation in the previous study.

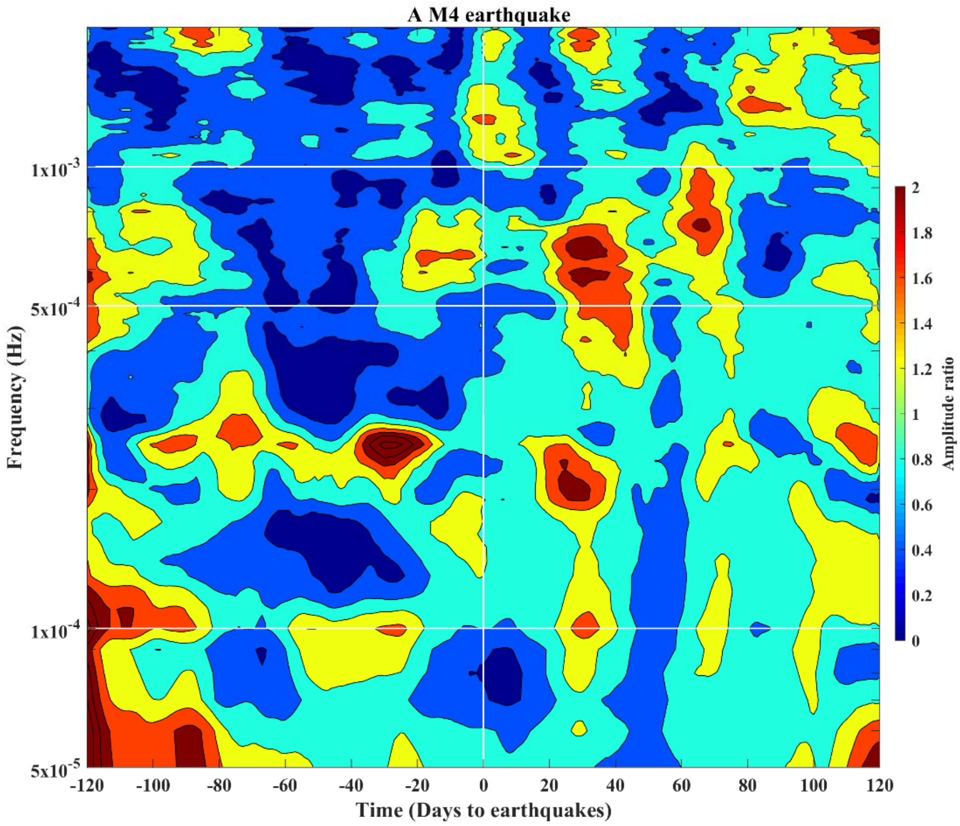

Fig. B. The amplitude ratios of the time-frequency-amplitude distribution of one M4.6 earthquake at (121.34E, 23.37N) in the Taiwan region on Dec. 12, 2015.

3) I am not totally convinced that the mechanism of resonance is the one responsible for the above observation. In my opinion this is a weaker point which can be also moved to supplementary, keeping a small discussion in the text.

Reply:

Thank you for the comments. The associated statements have been reduced (lines 296-310). The associated figure has been moved to the supplementary.

Summarizing, I believe that the direct analysis of seismic waveforms can contain more information than the one extracted from seismic catalogs. This is for instance shown in recent publications (Lippiello et al. Geophys. Res. Lett. and Lippiello et al. Nature Communications 2019). In this direction, the PCA method used by the authors is very promising. I invite the authors to a global rewriting of their manuscript in order to better stress the main results. I also invite the authors to perform the suggested or similar checks to support their findings.

Reply:

Thank you very much. These important recent publications have been cited in the revision. We have intensely rewritten the more than 50% statements in the manuscript. We have carefully performed the suggested or similar checks to support our findings.

Wide sensitive area of small foreshocks

Chieh-Hung Chen[1,2*], Yang-Yi Sun[2], Strong Wen[3], Peng Han[4], Li-Ching Lin[5], Huai-Zhong Yu[6], XueMin Zhang[7], Yongxin Gao[8], Chi-Chia Tang[1,2], Cheng-Horng Lin[9], Jann-Yenq Liu[10,11,12]

1. State Key Laboratory of Geological Processes and Mineral Resources, China University of Geosciences, Wuhan, China
2. Institute of Geophysics and Geomatics, China University of Geosciences, Wuhan, China
3. Department of Earth and Environmental Sciences, National Chung Cheng University, Chiayi, Taiwan
4. Department of Earth and Space Sciences, Southern University of Science and Technology, Shenzhen, China
5. National Applied Research Laboratories, Taipei, Taiwan
6. China Earthquake Networks Center, Beijing, China
7. Institute of Earthquake Forecasting, China Earthquake Administration, Beijing, China
8. School of Civil Engineering, Hefei University of Technology, Hefei, China
9. Institute of Earth Sciences, Academia Sinica, Taipei, Taiwan
10. Graduate Institute of Space Science, National Central University, Taoyuan, Taiwan
11. Center for Space and Remote Sensing Research, National Central University, Taoyuan, Taiwan
12. Center for Astronautical Physics and Engineering, National Central University, Taoyuan, Taiwan

*** Corresponding Author:**

Chieh-Hung Chen, E-mail: nononochchen@gmail.com

Institute of Geophysics and Geomatics,

China University of Geosciences, Wuhan, Hubei, 430074, China

Abstract

Scientists demystify stress changes within tens of days before a mainshock and often utilize its foreshocks as an indicator. Typically, foreshocks are detected near fault zones, which may be due to the distribution of seismometers. This study investigates changes in seismicity far from mainshocks by examining tens of thousands of M ≥ 2 quakes that were monitored by dense seismic arrays for more than 10 years in Taiwan and Japan. The quakes occurred within epicentral distances ranging from 0 km to 400 km during a period of 60 days before and after the mainshocks that are utilized to exhibit common behaviors of seismicity in the spatiotemporal domain. The superimposition results show that wide areas exhibit increased seismicity associated with mainshocks being more than 50 times to areas of the fault rupture. The seismicity increase initially concentrates in the fault zones, and gradually expands outward to over 50 km away from the epicenters approximately 40 days before the mainshocks. The seismicity increases more rapidly around the fault zones approximately 20 days before the mainshocks. The stressed crust triggers ground vibrations at frequencies varying from ~5×10^{-4} Hz to ~10^{-3} Hz (i.e., variable frequency) along with earthquake-related stress that migrates from exterior areas to approach the fault zones. The variable frequency is determined by the observation of continuous seismic waveforms through the superimposition processes and is further supported by the resonant frequency model. These results suggest that the variable frequency of ground vibrations is a function of areas with increased seismicity leading to earthquakes.

Keywords: foreshocks; resonance frequency; earthquake-related stressed area

1. Introduction

Numerous studies (Reasenberg, 1999; Scholz, 2002; Vidale et al., 2001; Ellsworth and Beroza, 1995) reported that foreshocks occur near a fault zone and migrate toward the hypocenter of a mainshock before its occurrence. The spatiotemporal evolution of foreshocks is generally considered to be an essential indicator that reveals variations in earthquake-related stress a couple of days before mainshocks. After detecting these variations, scientists installed multiple instruments along both sides of the fault over short distances to monitor the activity of the fault. However, these instruments typically detect small vibrations near the fault zone. Stress accumulates in a local region near a hypocenter triggering earthquake occurrence that is concluded from the sparse distribution of seismometers.

Bedford et al. (2020) analyzed the GNSS data and observed crustal deformation in a thousand-kilometer-scale area before the great earthquakes in the subduction zones. Chen et al. (2011, 2014, 2020a, 2020b) filtered the crustal displacements before earthquakes using the GNSS data through the Hilbert-Huang transform. The filtered crustal displacements in a hundred(thousand)-kilometer-scale area before the moderate-large (M9 Tohoku-Oki) earthquakes exhibit paralleling azimuths that yield an agreement with the most compressive axes of the forthcoming earthquakes. On the other hand, Dobrovolsky (1979) estimated the size of the earthquake preparation zone using the numerical simulation method and found that the radius (R) of the zone is proportional to earthquake magnitude (M). In addition, the relationship can be written by using a formula of $R=10^{0.43M}$. These results suggest that a stressed area before earthquakes is obviously larger than the rupture of fault zones. However, it is a big challenge to monitor stress changes in a wide area beneath the ground. A simple way to imagine this is if we place a stick on a table, then hold and try to break the stick. The stress we making on the stick can apply to either a limited local region or to both ends of it. Migrations and propagations of the loading force can be detected according to the changes of strain and the occurrence of microcracks. This common sense suggests that the spatiotemporal evolution of earthquake-related stress appearing a couple of days before mainshocks can be recognized if we can trace the occurrence of relatively-small quakes in a wide area (Kawamura et al., 2014; Wen and Chen, 2017). Here we take advantage of earthquake catalogs obtained by dense seismic arrays in

Taiwan and Japan to expose foreshocks distributing over a wide area instead of a local region.

2. Methodology

The ability to detect relatively-small quakes depends on the spatial density and capability of seismometers. Taiwan and Japan are both the most famous high-seismicity areas in the world. Dense seismometers evenly distributed throughout the whole area are beneficial for monitoring the earthquake occurrences near to and far away from fault zones (Chang, 2014). Earthquake catalogs retrieved from Taiwan and Japan were obtained from the Central Weather Bureau (CWB), Taiwan and the Japan Meteorological Agency (JMA), respectively. To distinguish dependencies from independent seismicity, the earthquake catalogs are declustered. Therefore, the ZMAP software package for MATLAB (Weimer, 2001) was utilized to remove and/or omit influence from duplicate events, such as aftershocks. The declustering algorithm used in ZMAP is based on the algorithm developed by Reasenberg (Reasenberg, 1985). We classify clusters by using the standard input parameters (proposed in Reasenberg, 1985 and Uhrhammer, 1986) for the declustering algorithm. Because the aftershock clusters in a small area and in a short period of time do not conform to the Poisson distribution, which requires removing the aftershocks from the earthquake sequence. Therefore, some parameters can be set as follow: The look-ahead time for un-clustered events is in one day, and the maximum look-ahead time for clustered events is in 10 days. The measure of probability to detect the next event in the earthquake sequence is 0.95. The effective minimum magnitude cut-off for the catalog is given by 1.5, and the interaction radius of dependent events is given by 10 km (van Stiphout et al., 2012). Earthquakes with depth > 30 km were eliminated from the declustered catalogs to understand seismicity changes before mainshocks mainly in the crust.

Before the analytical processes in this study, we assumed that earthquakes with relatively-small magnitude can be the cracks and potentially related to the far mainshocks based on the large seismogenic areas (Bedford et al., 2020). The minimum magnitudes of completeness Mc are 2.0 and 0.0 that can be determined by the declustered earthquake catalogs in Taiwan and Japan, respectively (also see Figs. S1–S4). The earthquakes with $M \geq 2$ are selected and utilized in this study for fair comparison of the seismicity changes during earthquakes in Taiwan and Japan. We classified the selected earthquakes via their magnitudes into three groups (i.e., $3 \leq M < 4$, $4 \leq M < 5$ and $5 \leq M < 6$). Note that the classified earthquakes in each group are determined as the break events (i.e., the mainshocks). In contrast, the other selected earthquakes with magnitudes smaller than the minima of the classified magnitude are determined as the crack events.

We construct a spatiotemporal distribution of the crack events for each break quake. The spatiotemporal distribution from 0 km to 400 km away from the epicenter of the break quake during a period of 60 days before and after the break occurrence is constructed to illustrate the relationship between the crack events and the break quake in the spatial and temporal domain. Note that the spatial and temporal resolutions of the grids of the spatiotemporal distribution are 10 km and 1 day, respectively, based on the declustering parameters in the ZMAP software (Weimer, 2001). We count the crack events in each spatiotemporal grid according to distance away from the epicenter and the differences in time before and after the occurrence of the break quake.

The superimposition process, a statistical tool utilized in data analysis, is capable of either detecting periodicities within a time sequence or revealing a correlation between more than two data sequences (Chree, 1913). The process is known as the superposed epoch analysis (Adams et al., 2003; Hocke, 2008). In practice, the superimposition is a process to stack numerous datasets that can migrate unique features for a few datasets and enhance common characteristics for the most datasets. The count in each grid of the spatiotemporal distributions for all the break quakes are superimposed as a total one based on the occurrence time and epicentral distance of the break quakes. The total count of the superimposed distribution in each spatiotemporal grid is normalized to seismic density (count/km^2) for comparing to the total number of the break quakes and the related spatial area. Moreover, we compute the average values every distance grid using the seismic densities 60 days before and after the quake. The average values are subtracted from the seismic densities and the obtained differences are divided by the average values in each distance grid to obtain the normalized variation clarifying changes of the seismic density in the spatiotemporal domain.

3. Analytical results

The earthquakes with magnitude ≥ 2 listed in the declustered catalogs of Taiwan from January 1991 to June 2017 are utilized to construct a spatiotemporal distribution of foreshocks and aftershocks corresponding to the quakes with 3 ≤ M < 4. We superimposed all the crack events corresponding to the 15625 quakes (3 ≤ M < 4). The seismic density is more than 1000 times greater in a hot region at a distance of 10 km away from an epicenter (which is generally considered to be the gestation area of foreshocks) than it is in areas located > 200 km from the epicenter (Fig. 1a). The sudden increase of seismic density suggests that earthquake-related stress accumulates mainly around the hot region, triggering many foreshocks a few days before the earthquakes with 3 ≤ M < 4. This partial agreement of the numerous recent studies reported that the seismicity migrates toward the fault rupture zone within tens of kilometers from epicenters a couple of days before earthquakes (Kato et al., 2012, Kato and Obara, 2014; Liu et al., 2019). Meanwhile, the events mainly occur 0–1 day after the quakes that is irrelevant to the smaller distribution 0–1 day before the quakes (also see Fig. 1). The seismic density close to epicenters (Fig. 1) suddenly increases before and gradually decreases after the quakes. The irrelevance and the differences of changes rates with epicentral distance smaller than 20 km before and after the quakes reveal that the increase of seismicity before the quakes is not contributed by the seismicity after due to the analytical processes in this study. In addition, these analytical results of the seismic activity are also in agreement with the studies in Lippiello et al. (2012, 2017, 2019) and de Arcangelis et al. (2016) regard for distinct methods.

On the other hand, the increase of seismic density is not only always limited within the hot region, but also extends outward to a distance of over 50 km away from the epicenters about 0–40 days leading up to the occurrence of the quakes (Fig. 1a). We further examine the spatiotemporal changes in the seismic density up to the M ≥ 4 quakes utilizing the same superimposition process (Figs. 1b–c). The expansion of the increased seismic density about 0–40 days leading up to the occurrence of the quakes and the sharp increases of seismic density a few days before the quakes that can be consistently observed using the M ≥ 4 quakes in Figs. 1b–c. Similar results (i.e., the sharp increases of seismic density a few days before the quakes and areas where the increase of the seismicity density is much larger than that of the hot region) can also be obtained using the earthquake catalogs between 2001 and 2010 from the Japan Meteorological Agency (JMA) in Japan (Figs. 1d–f). Note that the earthquakes that occurred in the northern side of the latitude of 32°N were selected from the Japan catalogs. The selection is based on that the earthquakes occurred in the area monitored by the dense seismometer network and to avoid the double count of events in the Taiwan catalogs. The normalized variations correspond to seismic density in Fig. 1 are shown in Fig. 2. The radii of the positive normalized variations are approximately 50 km while earthquake magnitude increases from 3 to 6 in Taiwan (Figs. 2a–c). The land area of Taiwan is approximately 250 km by 400 km, which causes underestimation of the seismic density in the spatial domain. In contrast, the positive normalized variations roughly expand along the radii ranging from 50 km to 150 km, while earthquake magnitude increases from 3 to 6 in Japan (Figs. 2d–f). However, variations in the lead time mostly range from 40 days to 20 days, and relationships between the positive normalized variations and the earthquake magnitude can be found neither in Taiwan nor Japan (Fig. 2).

In short, the expansion of the increase of seismic density becomes mitigation and may no longer be impact a place at distances > 200 km away from the epicenters for the earthquakes with magnitude < 6. The increase of seismicity density before the quakes suggests that the accumulation of the earthquake-related stress in the crust originates from the hot region, and gradually extends to an external place before earthquakes occur. The area of this external place is several times that of a fault rupture zone that is concluded based on the sparse seismic arrays of the past. If a quake can excite seismicity changes over a wide area (i.e., over 50 km by 50 km), any crustal vibration related to stress accumulation before earthquakes can be too small to be identified from continuous seismic waveforms at one station. In contrast, crustal vibrations can be a common characteristic of continuous seismic waveforms at most stations around fault zones due to that seismicity changes dominated by earthquake-related stress accumulation distributes in a wide area.

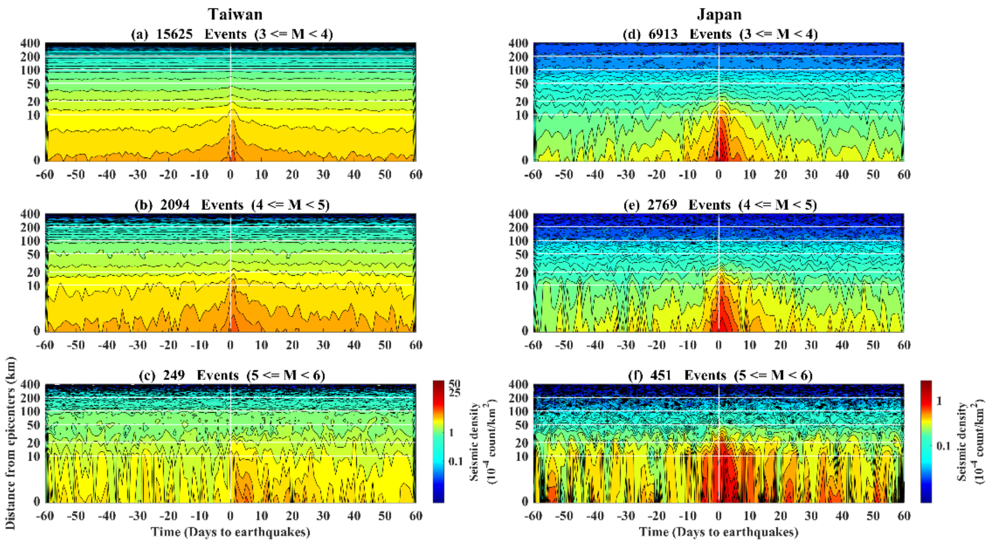

Fig. 1. Spatiotemporal seismic density distributions in Taiwan and Japan. The seismic densities constructed by using the declustered earthquake catalogs of Taiwan and Japan are shown in the left and right panels, respectively. The seismic density reveals changes in seismicity at distances from the epicenters ranging from 0 km to 400 km at up to 60 days before and after quakes in a particular magnitude group. The superimposed number in each grid is further normalized for a fair comparison by using the total number of quakes and their areas. Notably, the total number of quakes is shown in the title of each diagram.

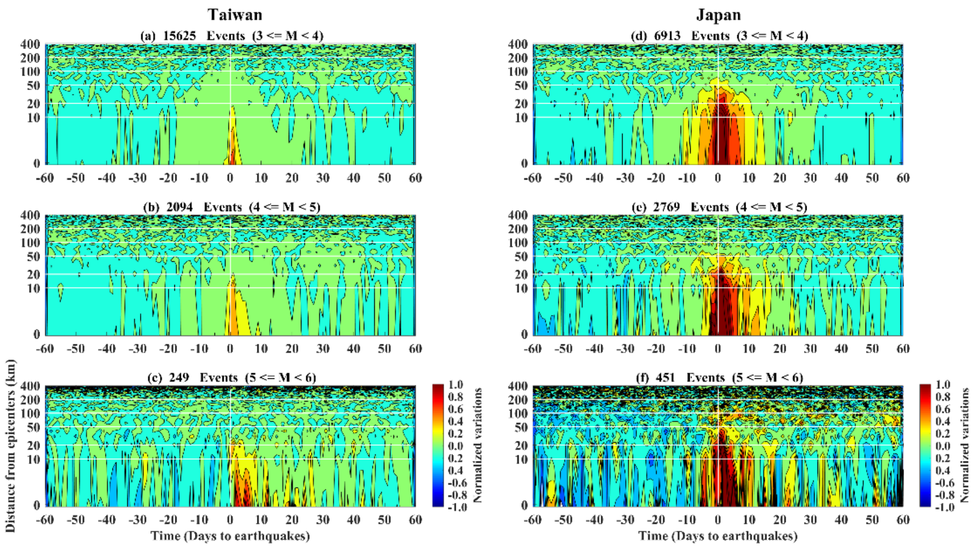

Fig. 2. Changes of the normalized spatiotemporal variations in Taiwan and Japan. The normalized variations correspond to the seismic density in Taiwan and Japan (in Fig. 1) are shown in the left and right panels, respectively. The colors reveal changes of the normalized variations at distances from the epicenters ranging from 0 km to 400 km at up to 60 days before and after quakes in a particular magnitude group.

4. The principal component analysis (PCA) on the continuous seismic waveforms

Seismic waveforms obtained from 33 broadband seismometers operated by National Center for Research on Earthquake Engineering (NCREE) of Taiwan, within a temporal span of approximately one year (from June 2015 to June 2016) are utilized in this study. Note that two seismometers of them are eliminated from following the analytical processes due to long data gaps. The principal component analysis (PCA) method (Jolliffe, 2002) is utilized to retrieve the possible stress-related common signals from continuous seismic waveforms on the vertical component at thirty-one seismic stations over a wide area and to mitigate local noise simultaneously. Fig. 3a shows that the energy and the cumulative energy of the principal components derived from the continuous seismic waveforms at the 31 stations. The energy of the first principal component is about 12% that is more than 3 times to the following ones. Thus, we determined the first principal component to be the common signals of the ground vibrations before earthquakes. Fig. 3b reveals changes in the common signals during the study period along the time. However, no obvious changes can be observed in the temporal domain.

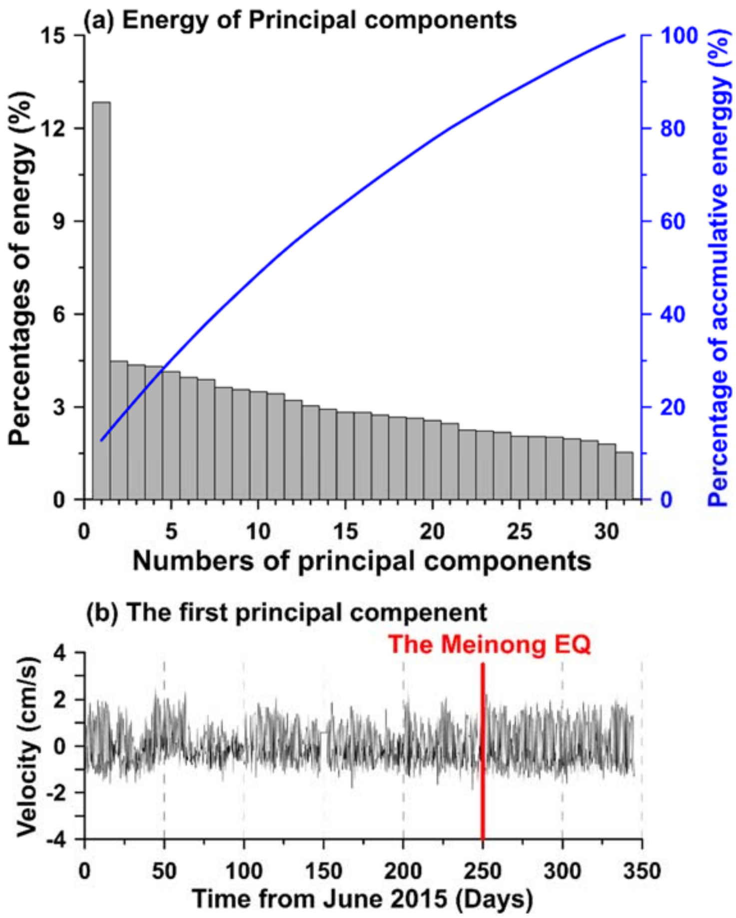

Fig. 3. The energy and the first principal component derived from vertical seismic velocity data from the 31 stations. The energy and the cumulative energy of the principal components are shown in (a). Bars denote the energy of each principal component. The blue line shows the variation of the cumulative energy from distinct used principal components. The variations of the first principal component during the period (i.e., from June 2015 to June 2016) are revealed in (b). The red vertical line indicates the occurrence time of the M6.6 Meinong earthquake (on February 2, 2016).

Thus, we sliced the common signals into several time spans using a 5-day moving window with one-day steps to show time-varying changes. The common signals in each time span are transferred into the frequency domain using the Fourier transform to investigate frequency characteristics of ground vibrations before earthquakes. The amplitudes are normalized using the frequency-dependent average values computed from the amplitude 30 days before and after earthquakes via the temporal division. Here, we take the M6.6 Meinong earthquake (Wen and Chen, 2017) as an example to understand the changes of the amplitude of the common signals in the spatiotemporal domain (Fig. 4a). Distinct patterns in the amplitude-frequency distributions can obviously be observed before and after the earthquake at frequency close to 5×10^{-4} Hz. The amplitude at the frequency close to 5×10^{-4} Hz was obviously enhanced approximately 20–40 days before the earthquake. Hereafter, the enhancements were significantly reduced and reached to a relatively-small value a few days after the earthquake. Meanwhile, the frequency is close to 5×10^{-4} Hz approximately 60 days before the earthquake and tends to be high near 10^{-3} Hz a few days before the event.

We next superimpose the amplitude based on the occurrence time of the 17 earthquakes with $4 \leq M < 5$ and the 109 earthquakes with $3 \leq M < 4$ during the one-year temporal span shown in Figs. 4b and 4c, respectively. The consistent variations (i.e., the frequency is close to 5×10^{-4} Hz approximately some days before the quakes tending to be high near 10^{-3} Hz a few days before the quakes) that can be observed in Figs. 4b and 4c. Note that the amplitudes of the variable frequency patterns are proportional to the earthquake magnitude. These results suggest that the common-mode ground vibrations exist in a wide area before earthquakes due to the signals being retrieved from the most stations distributing the whole Taiwan island through the PCA method. In short, the common-mode vibrations are very difficult to be identified from the time-series data but become significant in the frequency domain. If the expansion of the seismoeneric areas and the existence of the common-mode ground vibrations are true, the next step is to determine the potential mechanism hidden behind this nature.

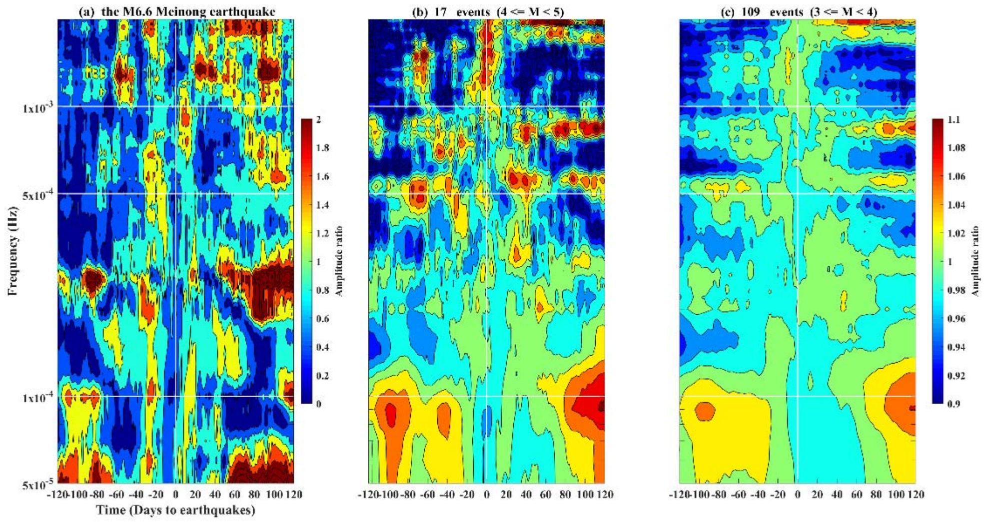

Fig. 4. The amplitude ratio of the superimposed time-frequency-amplitude distribution associated with earthquakes with distinct magnitudes. The superimposed results related to quakes with the M6.6 Meinong earthquake, $4 \leq M < 5$ and $3 \leq M < 4$ are shown in (a), (b) and (c), respectively. The distribution is normalized for comparison by using the average amplitude in each particular frequency band of 30 days before and after the quakes. The total number of earthquakes in each magnitude group is shown in the title of each diagram.

5. Discussions

Walczak et al. (2017) repeatedly observed stressed rocks exciting long-period vibrations during rock mechanics experiments. Leissa (1969) reported that the resonance frequency of an object is proportional to its Young's modulus and exhibits an inverse relationship to its mass. Based on the crust, the outermost of the Earth, is lamellar, we assume that the earthquake-related stress accumulates in the volume of a square sheet with a width of 100 km, which is determined by using a distance of 50 km away from an earthquake due to the significant increase of the seismic density (Figs. 1 and 2). The resonance frequency near 3×10^{-4} Hz (Fig. 4) can be derived from the square sheet once the thickness of the volume is ranged between 500 meters and 1000 meters (Fig. S5). Although we do not fully understand the causal mechanism of the thickness, the agreement with the spatiotemporal domain of the relatively-small quakes from the earthquake catalogs, the superimposition results of continuous seismic waveforms and the resonance frequency models suggest that the phenomenon of variable frequency may exist tens of days before earthquake occurrence and can be retrieved by broadband seismometers.

In this study, we determined the seismogenic areas using the relatively-small earthquakes in the spatiotemporal distribution and found that the areas are significantly larger than the fault rupture zone (Figs. 1 and 2). Meanwhile, the ground vibrations can exhibit frequency-dependent characteristics at about 10^{-4} Hz (Fig. 4) that could relate to the large seismogenic areas due to the resonance model (Fig. S5). If these are true, the seismo-TEC (total electron content) anomalies in the ionosphere, which is generally observed in a large-scale area with more than ten thousand square kilometers (Liu et al., 2009), are high potential to be driven by upward propagation of acoustic waves before earthquakes (Molchanov et al., 1998, 2011; Korepanov et al., 2009; Hayakawa et al., 2010, 2011; Sun et al., 2011; Oyama et al., 2016). The existence of the ground vibrations can generate the acoustic-gravity waves that have been reported (Liu et al., 2016, 2017). However, the acoustic-gravity waves in a period of < 300 seconds are difficult to propagate upward into the atmosphere and the ionosphere (Yeh and Liu, 1974; Azeem et al., 2018). The wide seismogenic areas observed in this study can contribute the larger-scale ground vibrations at approximately 5×10^{-4}–10^{-3} Hz that cover the frequency channel (< 1/300 Hz) for the acoustic-gravity waves propagating into the atmosphere and changing the TEC in the ionosphere. Meanwhile, the seismo-atmospheric and the seismo-ionospheric anomalies in a large-scale area can also be supported by the acoustic-gravity waves due to the wide seismogenic areas. While partial aforementioned relationships cannot be quickly proven, the ground vibrations at a low frequency (< 1/300 Hz) in a wide area assist our understanding of the essence of the seismo-anomalies in the atmosphere and the ionosphere.

6. Conclusion

The process of stress migration in the spatiotemporal domain can be concluded from tracing the increase of seismicity according to the 10-year earthquake catalogs from dense seismic arrays in Taiwan and Japan. Areas with the increase of seismicity, where stress accumulates in the crust triggering earthquakes are serious underestimation using a sparse seismic array. Seismicity initially increases around hypocenters, and this can be observed more than 50 days before quakes through superimposing large numbers of earthquakes. The seismicity gradually increases along with the expansion of areas from fault zones to an area widely covering an epicentral distance close to 50 km approximately 20–40 days before earthquakes. The crustal resonance exists at a frequency near 5×10^{-4} Hz when the expansion becomes insignificant. Instead of the spatial expansion, the sharp increase of seismicity around the hot regions suggests stress accumulation in fault zones generating crustal resonance at a frequency of up to $\sim10^{-3}$ Hz in the few days before earthquakes. Most broadband seismometers can observe the variable frequency of ground vibrations in Taiwan due to the comprehensive spatial coverage of resonant signals. The variable frequency depends on various stress-dominant areas that can be supported by the potential crustal resonance model. Seismic arrays comprise dense seismometers with a wide coverage are beneficial for monitoring the comprehensive process of stress migration in the spatiotemporal domain leading up to a faraway and forthcoming mainshock.

Acknowledgements. The authors appreciate scientists who devote to maintain instruments in the field and data centers in the office that leads chances to expose such interesting geophysical phenomena and understand potential processes during seismogenic periods. This research was funded by National Key R&D Program of China, grant number 2018YFC1503705; National Natural Science Foundation of China (Grants No. 41474038 and 41774048)； the Spark Program of Earthquake Science of China (Grant No. xh17045)； Ministry of Science and Technology of Taiwan (Grants No. MOST 106-2116-M-194-016- and MOST 106-2628-M-008-002), and Sichuan earthquake Agency-Research Team of GNSS based geodetic tectonophysics and mantle-crust dynamics of Chuan-Dian region (Grant No. 201803). Meanwhile, this work was also supported by the Center for Astronautical Physics and Engineering (CAPE) from the Featured Area Research Center program within the framework of Higher Education Sprout Project by the Ministry of Education (MOE) in Taiwan.

References

Adams, J.B., Mann, M.E., and Ammann, C.M.: Proxy evidence for an El Niño-like response to volcanic forcing, Nature, 426, 274–278, 2003.

Azeem, I., Walterscheid, R. L. and Crowley, G.: Investigation of acoustic waves in the ionosphere generated by a deep convection system using distributed networks of GPS receivers and numerical modeling, Geophys. Res. Lett., 45, 8014–8021, 2018.

Bedford, J.R., Moreno, M., Deng, Z. et al.: Months-long thousand-kilometre-scale wobbling before great subduction earthquakes, Nature, 580, 628–635, 2020.

Chang, C.H.: Introduction to the Meteorological Bureau Earthquake Monitoring Network, Taiwan Earthquake Research Center Newsletter, 2014.

Chen, C.-H., Yeh, T.-K., Wen, S., Meng, G., Han, P., Tang, C.-C., Liu, J.-Y. and Wang, C.-H.: Unique Pre-Earthquake Deformation Patterns in the Spatial Domains from GPS in Taiwan, Remote Sens., 12, 366, 2020a.

Chen, C.-H., Su, X., Cheng, K.-C., Meng, G., Wen, S., Han, P., Tang, C.-C., Liu, J.-Y. and Wang, C.-H.: Seismo-deformation anomalies associated with the M6.1 Ludian earthquake on August 3, 2014, Remote Sens., 12, 1067, 2020b.

Chen, C.H., Wen, S., Liu, J.Y., Hattori, K., Han, P., Hobara, Y., Wang, C.H., Yeh, T.K. and Yen, H.Y.: Surface displacements in Japan before the 11 March 2011 M9.0 Tohoku-Oki earthquake, J. Asian Earth Sci., 80, 165–171, 2014.

Chen, C.H., Yeh, T.K., Liu, J.Y., Wang, C.H., Wen, S., Yen, H.Y. and Chang, S.H.: Surface Deformation and Seismic Rebound: implications and applications, Surv. Geophys., 32(3), 291–313, 2011.

Chree, C.: Some phenomena of sunspots and of terrestrial magnetism at Kew observatory, Phil. Trans. R. Soc., 212, 75, 1913.

de Arcangelis, L., Godano, C., Grasso, J.R. and Lippiello, E.: Statistical physics approach to earthquake occurrence and forecasting, Phys. Rep., 628, 1–91, 2016.

Dobrovolsky, I.P., Zubkov, S.I. and Miachkin, V.I.: Estimation of the size of earthquake preparation zones, Pure Appl. Geophys., 117, 1025–1044, 1979.

Ellsworth, W.L., and Beroza, G.C.: Seismic evidence for an earthquake nucleation phase, Science, 268, 851–855, 1995.

Hayakawa, M., Kasahara, Y., Nakamura, T., Hobara, Y., Rozhnoi, A., Solovieva, M., Molchanov, O. and Korepanov, V.: Atmospheric gravity waves as a possible candidate for seismo-ionospheric perturbations, J.Atmos. Electr., 31, 129–140, 2011.

Hayakawa, M.， Kasahara, Y., Nakamura, T., Muto, F., Horie, T., Maekawa, S., Hobara, Y., Rozhnoi, A.A., Solovieva, M. and Molchanov, O.A.: A statistical study on the correlation between lower ionospheric perturbations as seen by subionospheric VLF/LF propagation and earthquakes, J. Geophys. Res., 115, A09305, 2010,

Hocke, K., Oscillations of global mean TEC, J. Geophys. Res., 113, A04302, https://doi.org/10.1029/2007JA012798, 2008.

Jolliffe, I.T.: Principal Component Analysis, second edition, Springer, 2002.

Kato, A., and Obara, K.: Step-like migration of early aftershocks following the 2007 M_W 6.7 Noto-Hanto earthquake, Japan, Geophys. Res. Lett., 41, 3864–3689, https://doi.org/10.1002/2014GL060427, 2014.

Kato, A., Obara, K., Igarashi, T., Tsuruoka, H., Nakagawa, S., and Hirata, N.: Propagation of slow slip leading up to the 2011 M_W9.0 Tohoku-Oki earthquake, Science, 335, 705–708, https://doi.org/10.1126/science.1215141， 2012.

Kawamura, M., Chen, C.C., and Wu, Y.M.: Seismicity change revealed by ETAS, PI, Z-value methods: A case study of the 2013 Nantou, Taiwan earthquake, Tectonophysics, 634, 139–155， 2014.

Korepanov, V., Hayakawa, M., Yampolski, Y., Lizunov, G.: AGW as a seismo-ionospheric coupling responsible agent, Phys. Chem. Earth, 34, 485–495, 2009.

Leissa, A.W., Vibrations of plates. Ohio State University, Columbus, Ohio, 1969.

Lippiello, E., Giacco, F., Marzocchi, W., Godano, C. and Arcangelis, L.D.: Statistical Features of Foreshocks in Instrumental and ETAS Catalogs, Pure Appl. Geophys., 174, 1679–1697, 2017.

Lippiello, E., Godano, C. and de Arcangelis, L.: The Relevance of Foreshocks in Earthquake Triggering: A Statistical Study, Entropy, 21, 173, 2019.

Lippiello, E., Marzocchi, W., de Arcangelis, L. and Godano, C.: Spatial organization of foreshocks as a tool to forecast large earthquakes, Sci. Rep., 2, 846, 2012.

Liu, J.Y., Chen, C.H., Sun, Y.Y., Chen, C.H., Tsai, H.F., Yen, H.Y., Chum, J., Lastovicka, J., Yang, Q.S., Chen, W.S. and Wen, S.: The vertical propagation of disturbances triggered by seismic waves of the 11 March 2011 M9.0 Tohoku Earthquake over Taiwan, Geophys. Res. Lett., 43, 1759–1765, 2016.

Liu, J.Y., Chen, C.H., Wu, T.Y., Chen, H.C., Hattori, K., Bleier, T., Kappler, K., Yang, I.C., Xia, Y., Chen, W. and Liu, Z.: Co-seismic signatures in magnetometer, geophone, and infrasound data during the Meinong Earthquake, Terr. Atmos. Ocean Sci., 28(5), 683–692, 2017.

Liu, J.Y., et al.: seismoionospheric GPS total electron content anomalies observed before the 12 May 2008 Mw 7.9 Wenchuan earthquake, J. Geophys. Res., 114, A04320, 2009.

Liu, S., Tang, C.C., Chen, C.H., and Xn, R.: Spatiotemporal Evolution of the 2018 Mw 6.4 Hualien Earthquake Sequence in Eastern Taiwan, Seismol. Res. Lett., https://doi.org/10.1785/0220180389， 2019.

Molchanov, O.A., and Hayakawa, M.: Subionospheric VLF signal perturbations possibly related to earthquakes, J. Geophys. Res. Space Phys., 103, 17489–17504, 1998.

Molchanov, O.A., Hayakawa, M. and Miyaki, K.: VLF/LF sounding of the lower ionosphere to study the role of atmospheric oscillations in the lithosphere-ionosphere coupling, Adv. Polar Up. Atmos. Res., 15, 146–158, 2011.

Oyama, K.-I., Devi, M., Ryu, K., Chen, C.-H., Liu J.-Y., Liu, H., Bankov, L. and

Kodama, T.: Modifications of the ionosphere prior to large earthquakes: report from the Ionosphere Precursor Study Group, GeoSci. Lett., 3–6, 2016.

Reasenberg, P.： Second-order moment of central California seismicity, 1969-82, J. Geophys. Res., 90, 5479–5495, 1985.

Reasenberg, Paul A.: Foreshock occurrence before large earthquakes, J. Geophys. Res., 104, 4755–4768, 1999.

Scholz, C.H.： The Mechanics of Earthquakes and Faulting. second edition, Cambridge University Press, Cambridge, UK, 2002.

Sun, Y.Y., Oyama, K.-I., Liu, J.Y., Jhuang, H.K. and Cheng, C.Z.: The neutral temperature in the ionospheric dynamo region and the ionospheric F region density during Wenchuan and Pingtung Doublet earthquakes, Nat. Hazards Earth Syst. Sci., 11, 1759–1768, 2011.

Uhrhammer, R.: Characteristics of northern and southern California seismicity: Earthquake Notes, 57, 21, 1986.

van Stiphout, T., Zhuang, J. and Marsan, D.: Seismicity declustering, Community Online Resource for Statistical Seismicity Analysis, 2012, doi:10.5078/corssa52382934. Available at http://www.corssa.org.

Vidale, J., Mori, J.， and Houston, H.: Something wicked this way comes: Clues from foreshocks and earthquake nucleation, Eos Trans. AGU, 82, 68, 2001.

Walczak, P. et al.: Real time observation of granular rock analogue material deformation and failure using nonlinear laser interferometry, arXiv preprint, arXiv:1705.03377v1, 2017.

Wen, Y.-Y., and Chen, C.-C.: Seismicity variations prior to the 2016 ML 6.6 Meinong, Taiwan earthquake, Terr. Atmos. Ocean. Sci., 28, 739–744, https://doi.org/10.3319/ TAO.2016.12.05.01, 2017.

Wiemer, S.: A Software Package to Analyze Seismicity: ZMAP, Seismol. Res. Lett., 72, 373–382, https://doi.org/10.1785/gssrl.72.3.373, 2001.

Yeh, K.C. and Liu, C.H.: Acoustic-gravity waves in the upper atmosphere, Rev.

Geophys., 12(2), 193– 212, 1974.

Data available

The earthquake catalogs of Taiwan and Japan were obtained from the Central Weather Bureau (https://www.cwb.gov.tw/), and the Japan Meteorological Agency (JMA; https://www.jma.go.jp/jma/indexe.html), respectively. Seismic waveform data in Taiwan were provided by the Seismic Array of NCREE in Taiwan (SANTA; https://www.ncree.narl.org.tw/; please find the bottom for the English version in the top right side). The downsampled seismic waveforms with the temporal interval of 10 seconds can be utilized to reproduce the analytical results in this study through the MATLAB software that can be download at https://doi.org/10.5061/dryad.1jwstqjqq.

Author contribution

Y.Y.S. contributed discussion and revision; S.W. contributed discussion and revision; P.H. contributed data collection; L.C.L. contributed discussion and revision; H.Z.Y. contributed discussion; X.Z. contributed discussion; Y.G. contributed discussion; C.C.T. contributed discussion and revision; C.H.L. contributed discussion and revision; J.Y.L. contributed discussion and revision.

Competing interests

The authors declare that they have no known competing financial interests or personal relationships that could have appeared to influence the work reported in this paper.